Ray tracing of black hole with astrometric and aberration of light

朱庆华，重庆大学

ArXiv: 2311.17390

—

PhysRevD.101.084029,
PhysRevD.102.044012,
doi.org/10.1088/1475-7516/2021/09/003

2023-12-3, 黑洞图像学术研讨会，北京

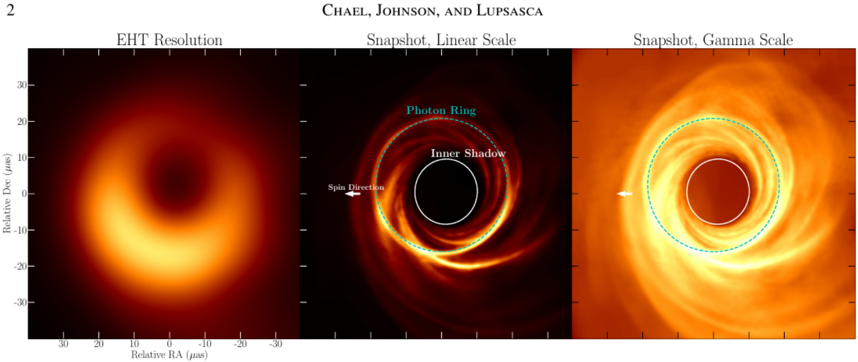

A. Chael et al. ApJ 2021.

Introduction

Order of Images

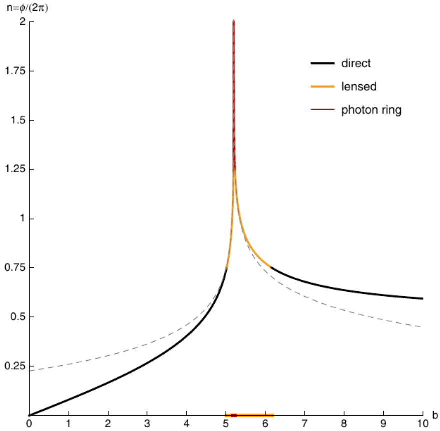

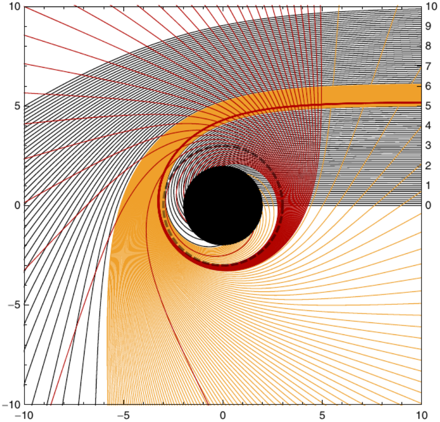

S. E. Gralla. PRD 2019.

K. S. Virbhadra & G. F. R. Ellis, PRD 1999 *call them primary, secondary and relativistic images

Introduction

Shadow versus Center Dark region

F. H. Vincent et al.: Images and photon ring signatures of thick disks around black holes

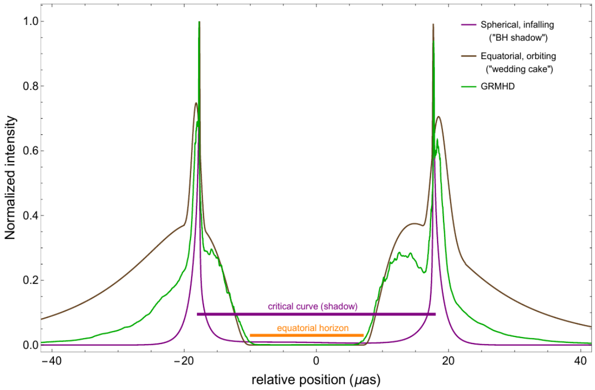

F. H. Vincent et al. A&A 2022.

- 光源 — 黑洞 — 观者
- 对成像结果的影响：光源 $>$ 黑洞 $>$ 观者

Motivation

- 光源 — 黑洞 — 观者
- 对成像结果的影响：光源 > 黑洞 > 观者
- 理论的研究兴趣：黑洞 > 光源 > 观者

- 光源 — 黑洞 — 观者
- 对成像结果的影响：光源 > 黑洞 > <u>观者</u>
- 理论的研究兴趣：黑洞 > 光源 > <u>观者</u>

THE APPARENT SHAPE OF A RELATIVISTICALLY MOVING SPHERE

By R. PENROSE

Received 29 July 1958

It would be natural to assume that, according to the special theory of relativity, an object moving with a speed comparable with that of light should *appear* to be flattened in the direction of motion on account of its FitzGerald–Lorentz contraction. It will be shown here, however, that this is by no means generally the case. It turns out, in particular, that the appearance of a sphere, no matter how it is moving, is always such as to present a *circular* outline to any observer. Thus an instantaneous photograph* of a rapidly moving sphere has the same outline as that of a stationary sphere.

THE APPARENT SHAPE OF A RELATIVISTICALLY MOVING SPHERE

By R. PENROSE

Received 29 July 1958

It would be natural to assume that, according to the special theory of relativity, an object moving with a speed comparable with that of light should *appear* to be flattened in the direction of motion on account of its FitzGerald–Lorentz contraction. It will be shown here, however, that this is by no means generally the case. It turns out, in particular, that the appearance of a sphere, no matter how it is moving, is always such as to present a *circular* outline to any observer. Thus an instantaneous photograph* of a rapidly moving sphere has the same outline as that of a stationary sphere.

$$\tan\Psi' = \tan\Psi\sqrt{\frac{1-v}{1+v}}$$

Motivation

Significant Aberration: Co-moving observers (2/3)

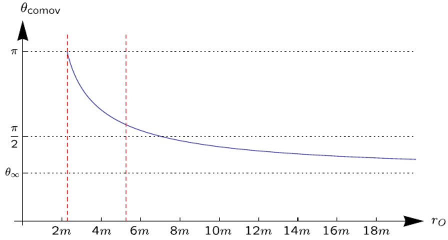

Perlick et al. PRD, 2018

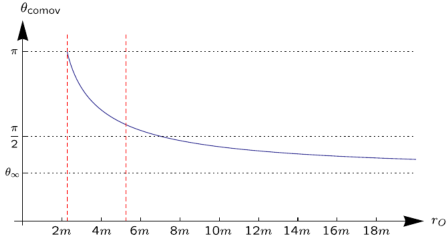

Perlick et al. PRD, 2018

$$\sin\psi|_{r=\infty} = 3M\sqrt{\Lambda}\ .$$

Motivation

Significant Aberration: Co-moving observers (2/3)

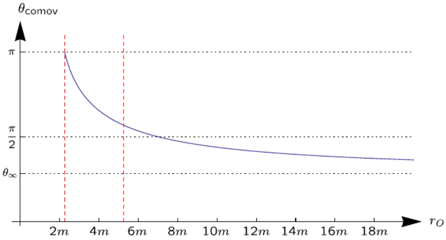

Perlick et al. PRD, 2018

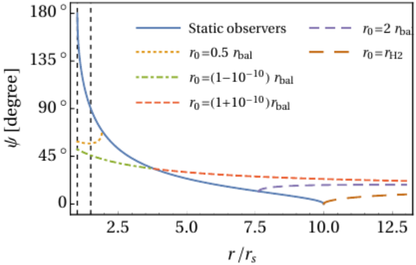

Chang & Zhu JCAP, 2020

$$\sin\psi|_{r=\infty} = 3M\sqrt{\Lambda}\ .$$

Distortion parameter: $\delta = 1 - D_{\max}/D_{\min}$

Bardeen, 1972
Grenzebach et al. 2014
Chang & Zhu. PRD, 2020

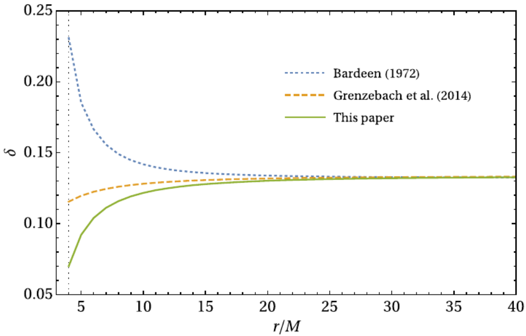

Distortion parameter: $\delta = 1 - D_{\text{max}}/D_{\text{min}}$

Bardeen, 1972

Grenzebach et al. 2014

Chang & Zhu. PRD, 2020

- The aberration formula is well-defined in flat space-time.

- The aberration formula is well-defined in flat space-time.
- Aberration is not always small

- The aberration formula is well-defined in flat space-time.
- Aberration is not always small
- Choice of tetrad/local frame/moving frame will result in aberration effect

- The aberration formula is well-defined in flat space-time.
- Aberration is not always small
- Choice of tetrad/local frame/moving frame will result in aberration effect

Naive: influence on black hole images

Imaging and Observers' Celestial Sphere

Locating light ray without tetrad

Local frame/Tetrad

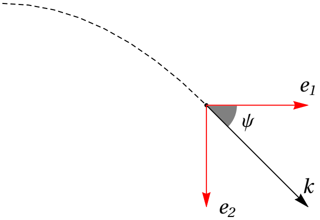

Local frame/Tetrad

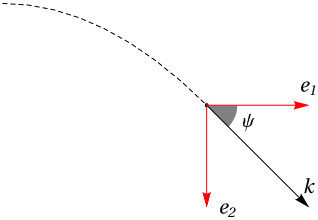

$$\psi = \arctan\left(\frac{k^{(2)}}{k^{(1)}}\right)$$

Imaging and Observers' Celestial Sphere

Locating light ray without tetrad

Local frame/Tetrad

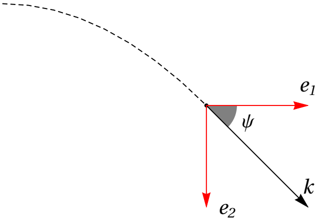

$$\psi = \arctan\left(\frac{k^{(2)}}{k^{(1)}}\right)$$

Astrometric observables

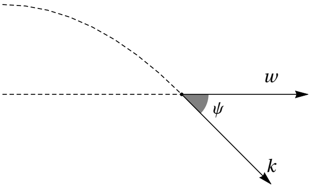

Soffel & Han (2019)

Local frame/Tetrad

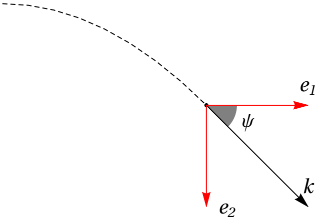

$$\psi = \arctan\left(\frac{k^{(2)}}{k^{(1)}}\right)$$

Astrometric observables

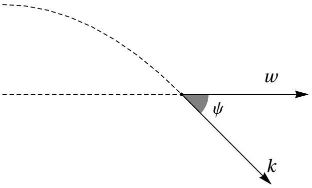

$$\psi = \arccos\left(\frac{\gamma^* k \cdot \gamma^* w}{|\gamma^* k||\gamma^* w|}\right)$$

Soffel & Han (2019)

Imaging and Observers' Celestial Sphere

Astrometric Approach

Imaging and Observers' Celestial Sphere

Astrometric Approach

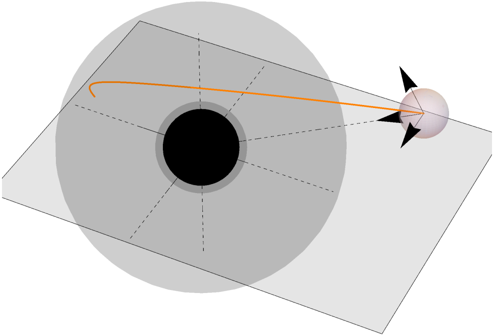

Using tetrad

Imaging and Observers' Celestial Sphere

Astrometric Approach

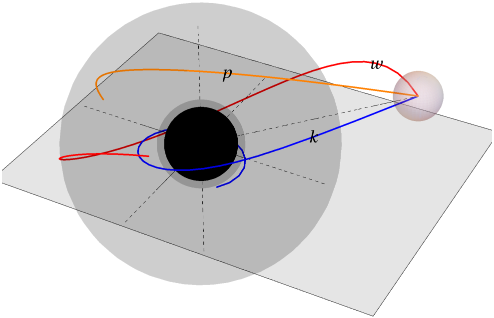

Using astrometric observables

Imaging and Observers' Celestial Sphere

Astrometric Approach

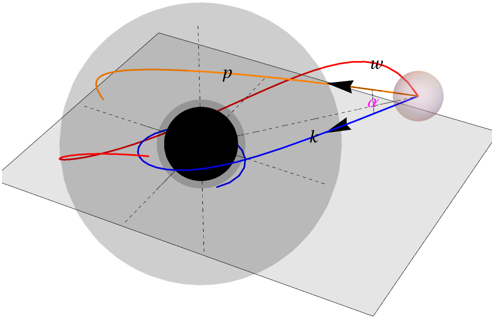

Using astrometric observables

Imaging and Observers' Celestial Sphere

Astrometric Approach

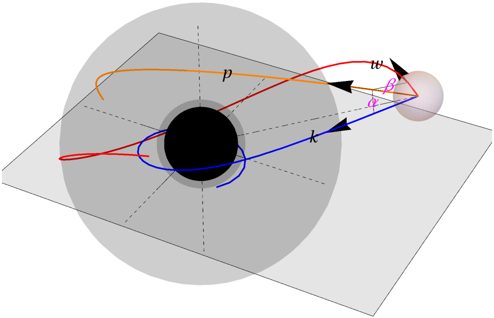

Using astrometric observables

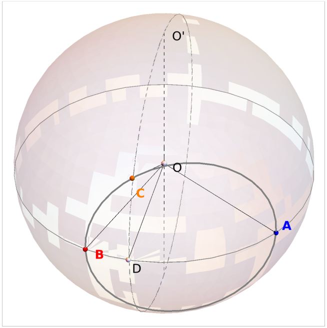

$\alpha = \angle COA$
$\beta = \angle COB$
$\gamma = \angle AOB$
$\Phi = \angle BOD$
$\Psi = \angle O'OC$

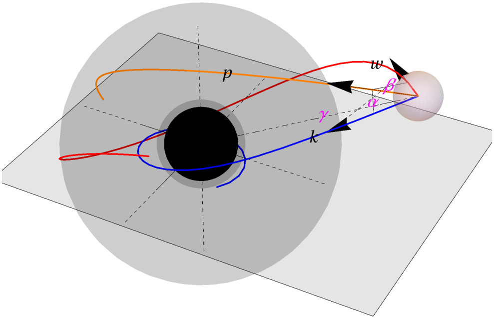

Using astrometric observables

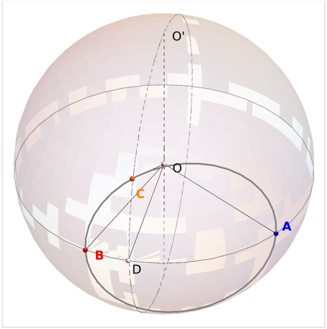

$\alpha = \angle COA$
$\beta = \angle COB$
$\gamma = \angle AOB$
$\Phi = \angle BOD$
$\Psi = \angle O'OC$

Celestial coordinate:

$$\Psi = \arccos\left(\sin\beta\sqrt{1-\left(\frac{\cos\alpha-\cos\beta\cos\gamma}{\sin\beta\sin\gamma}\right)^2}\right),$$

$$\Phi = \arccos\left(\frac{\cos\beta}{\sin\Psi}\right),$$

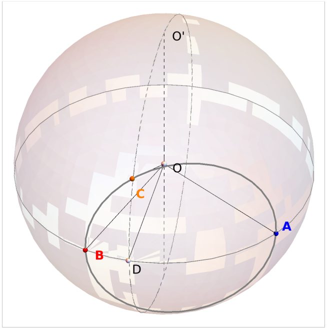

$\alpha = \angle COA$
$\beta = \angle COB$
$\gamma = \angle AOB$
$\Phi = \angle BOD$
$\Psi = \angle O'OC$

Celestial coordinate:

$$\Psi = \arccos\left(\sin\beta\sqrt{1-\left(\frac{\cos\alpha-\cos\beta\cos\gamma}{\sin\beta\sin\gamma}\right)^2}\right),$$

$$\Phi = \arccos\left(\frac{\cos\beta}{\sin\Psi}\right),$$

criterion:

$$\Upsilon = \mathrm{sign}(\cos\delta - \cos(\Phi-\Phi_l)\sin\Psi\sin\Psi_l),$$

where $\delta = \mathrm{Angle}(p, l)$, $\Phi_l \equiv \Psi|_{p=l}$ and $\Psi_l \equiv \Psi|_{p=l}$.

Shadow for Observers in Motions

Hint 1: For near and distant equatorial observers.

Chang & Zhu, PRD, 2020

Shadow for Observers in Motions

Hint 1: For near and distant equatorial observers.

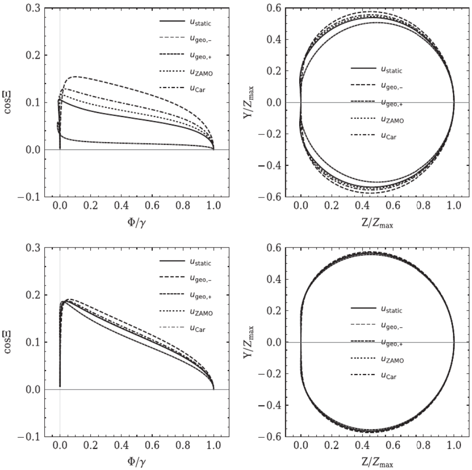

Chang & Zhu, PRD, 2020

Shadow for Observers in Motions

Hint 1: For near and distant equatorial observers.

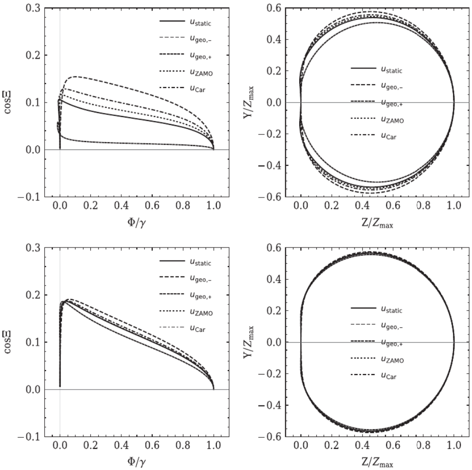

$$r_{\rm obs} = 4M\ , \quad \theta_{\rm obs} = \pi/2\ .$$

Chang & Zhu, PRD, 2020

Shadow for Observers in Motions

Hint 1: For near and distant equatorial observers.

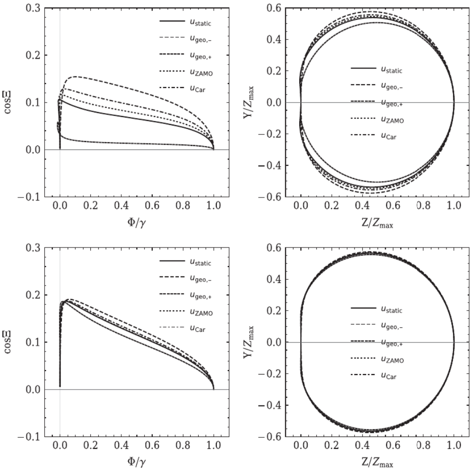

$$r_{\rm obs} = 4M\,, \quad \theta_{\rm obs} = \pi/2\;.$$

$$r_{\rm obs} = 14M\,, \quad \theta_{\rm obs} = \pi/2\,.$$

Chang & Zhu, PRD, 2020

Shadow for Observers in Motions

Hint 2: axial motion along θ-coordinate

Chang & Zhu, JCAP, 2021

Hint 2: axial motion along θ-coordinate

$$u^{(\theta,+)} = \frac{\mathcal{E}}{N^2}\partial_t + \frac{\sqrt{\Delta_\theta}}{B}\sqrt{\left(\frac{\mathcal{E}}{N}\right)^2 - 1}\partial_\theta \ ,$$

Chang & Zhu, JCAP, 2021

Shadow for Observers in Motions

Hint 2: axial motion along θ-coordinate

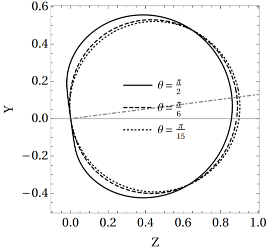

$$u^{(\theta,+)} = \frac{\mathcal{E}}{N^2}\partial_t + \frac{\sqrt{\Delta_\theta}}{B}\sqrt{\left(\frac{\mathcal{E}}{N}\right)^2 - 1}\partial_\theta \ ,$$

Chang & Zhu, JCAP, 2021

Shadow for Observers in Motions

Hint 2: axial motion along θ-coordinate

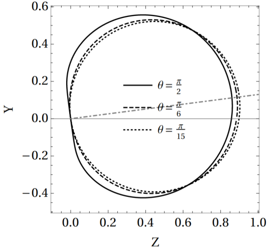

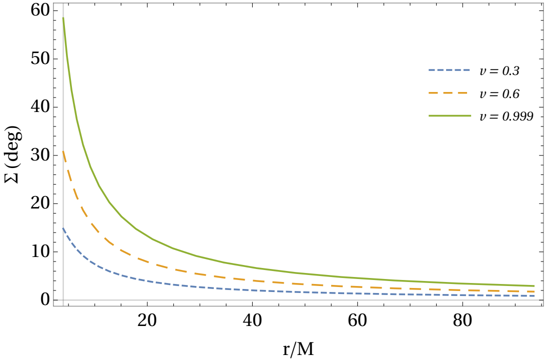

$$u^{(\theta,+)} = \frac{\mathcal{E}}{N^2}\partial_t + \frac{\sqrt{\Delta_\theta}}{B}\sqrt{\left(\frac{\mathcal{E}}{N}\right)^2 - 1}\partial_\theta \ ,$$

Chang & Zhu, JCAP, 2021

- Does the gravity environment affect the imaging of a black hole?

Geodesic equations

Transfer Equations for Kerr-de Sitter black hole

Mino time:

$$\tau \equiv G_\theta(\theta_{\rm o},\theta_{\rm s}) = \mathcal{G}_\theta(\theta_{\rm o}) - \mathcal{G}_\theta(\theta_{\rm s}) \ ,$$

Mino time:

$$\tau \equiv G_\theta(\theta_\mathrm{o}, \theta_\mathrm{s}) = \mathcal{G}_\theta(\theta_\mathrm{o}) - \mathcal{G}_\theta(\theta_\mathrm{s}) \ ,$$

Transfer functions:

$$\begin{aligned} r_\mathrm{s} &= I_r^{-1}(r_\mathrm{o}; \tau) \ , \\ \phi_\mathrm{s} &= \phi_\mathrm{o} - I_\phi(r_\mathrm{o}, r_\mathrm{s}) - \lambda G_\phi(\theta_\mathrm{o}, \theta_\mathrm{s}) \\ &\quad - \frac{\Lambda}{3} a^3 G_t(\theta_\mathrm{o}, \theta_\mathrm{s}) \ , \\ t_\mathrm{s} &= t_\mathrm{o} - I_t(r_\mathrm{o}, r_\mathrm{s}) \\ &\quad - a^2 \left(1 + \frac{\Lambda}{3}(a^2 - a\lambda)\right) G_t(\theta_\mathrm{o}, \theta_\mathrm{s}) \ , \end{aligned}$$

where $I_*(r_\mathrm{o}, r_\mathrm{s}) \equiv \mathcal{I}_*(r_\mathrm{s}) - \mathcal{I}_*(r_\mathrm{o}),\ G_*(\theta_\mathrm{o}, \theta_\mathrm{s}) \equiv \mathcal{G}_*(\theta_\mathrm{s}) - \mathcal{G}_*(\theta_\mathrm{o}),$

Mino time:

$$\tau \equiv G_\theta(\theta_o, \theta_s) = \mathcal{G}_\theta(\theta_o) - \mathcal{G}_\theta(\theta_s) \ ,$$

Transfer functions:

$$\begin{aligned} r_s &= I_r^{-1}(r_o; \tau) \ , \\ \phi_s &= \phi_o - I_\phi(r_o, r_s) - \lambda G_\phi(\theta_o, \theta_s) \\ &\quad -\frac{\Lambda}{3} a^3 G_t(\theta_o, \theta_s) \ , \\ t_s &= t_o - I_t(r_o, r_s) \\ &\quad -a^2 \left(1 + \frac{\Lambda}{3}(a^2 - a\lambda)\right) G_t(\theta_o, \theta_s) \ , \end{aligned}$$

and

$$\begin{aligned} \mathcal{I}_r(r) &\equiv \pm_r \int \frac{\mathrm{d}r}{\sqrt{\mathcal{R}(r)}} \ , \\ \mathcal{I}_t(r) &\equiv \pm_r \int \mathrm{d}r \left\{ \frac{r^2\Delta_r + \left(\frac{1}{3}\Lambda r^2(r^2+a^2) + 2Mr\right)(r^2 + a^2 - a\lambda)}{\Delta_r\sqrt{\mathcal{R}(r)}} \right\} \ , \\ \mathcal{I}_\phi(r) &\equiv \pm_r \int \mathrm{d}r \left\{ \frac{a\left(2Mr - a\lambda - \frac{1}{3}\Lambda r^2(r^2+a^2)\right)}{\Delta_r\sqrt{\mathcal{R}(r)}} \right\} \ , \\ \mathcal{G}_\theta(\theta) &\equiv \pm_\theta \int \frac{\mathrm{d}\theta}{\sqrt{\Theta(\theta)}} \ , \\ \mathcal{G}_t(\theta) &\equiv \pm_\theta \int \mathrm{d}\theta \left\{ \frac{\cos^2\theta}{\Delta_\theta\sqrt{\Theta(\theta)}} \right\} \ , \\ \mathcal{G}_\phi(\theta) &\equiv \pm_\theta \int \mathrm{d}\theta \left\{ \frac{\csc^2\theta}{\Delta_\theta\sqrt{\Theta(\theta)}} \right\} \ . \end{aligned}$$

where $I_*(r_o, r_s) \equiv \mathcal{I}_*(r_s) - \mathcal{I}_*(r_o)$, $G_*(\theta_o, \theta_s) \equiv \mathcal{G}_*(\theta_s) - \mathcal{G}_*(\theta_o)$,

Mino time:

$$\tau \equiv G_\theta(\theta_o, \theta_s) = \mathcal{G}_\theta(\theta_o) - \mathcal{G}_\theta(\theta_s) \ ,$$

Transfer functions:

$$\begin{aligned} r_s &= I_r^{-1}(r_o; \tau) \ , \\ \phi_s &= \phi_o - I_\phi(r_o, r_s) - \lambda G_\phi(\theta_o, \theta_s) \\ &\quad - \frac{\Lambda}{3} a^3 G_t(\theta_o, \theta_s) \ , \\ t_s &= t_o - I_t(r_o, r_s) \\ &\quad - a^2 \left(1 + \frac{\Lambda}{3}(a^2 - a\lambda)\right) G_t(\theta_o, \theta_s) \ , \end{aligned}$$

and

$$\begin{aligned} \mathcal{I}_r(r) &\equiv \pm_r \int \frac{\mathrm{d}r}{\sqrt{\mathcal{R}(r)}} \ , \\ \mathcal{I}_t(r) &\equiv \pm_r \int \mathrm{d}r \left\{ \frac{r^2\Delta_r + \left(\frac{1}{3}\Lambda r^2(r^2+a^2) + 2Mr\right)(r^2+a^2-a\lambda)}{\Delta_r\sqrt{\mathcal{R}(r)}} \right\} \ , \\ \mathcal{I}_\phi(r) &\equiv \pm_r \int \mathrm{d}r \left\{ \frac{a\left(2Mr - a\lambda - \frac{1}{3}\Lambda r^2(r^2+a^2)\right)}{\Delta_r\sqrt{\mathcal{R}(r)}} \right\} \ , \\ \mathcal{G}_\theta(\theta) &\equiv \pm_\theta \int \frac{\mathrm{d}\theta}{\sqrt{\Theta(\theta)}} \ , \\ \mathcal{G}_t(\theta) &\equiv \pm_\theta \int \mathrm{d}\theta \left\{ \frac{\cos^2\theta}{\Delta_\theta\sqrt{\Theta(\theta)}} \right\} \ , \\ \mathcal{G}_\phi(\theta) &\equiv \pm_\theta \int \mathrm{d}\theta \left\{ \frac{\csc^2\theta}{\Delta_\theta\sqrt{\Theta(\theta)}} \right\} \ . \end{aligned}$$

where $I_*(r_o, r_s) \equiv \mathcal{I}_*(r_s) - \mathcal{I}_*(r_o)$, $G_*(\theta_o, \theta_s) \equiv \mathcal{G}_*(\theta_s) - \mathcal{G}_*(\theta_o)$,

Emission intensity

$$I_{\mathrm{emt}}(\boldsymbol{x}) = \begin{cases} f_{\mathsf{d}}(r)\Theta\left(r_{\mathsf{d},+} - r\right)\Theta\left(r - r_{\mathsf{d},-}\right) & \theta = \frac{\pi}{2} \\ 0 & \theta \neq \frac{\pi}{2} \end{cases}$$

Emission intensity

$$I_{\mathrm{emt}}(\boldsymbol{x}) = \begin{cases} f_{\mathsf{d}}(r)\Theta\left(r_{\mathsf{d},+} - r\right)\Theta\left(r - r_{\mathsf{d},-}\right) & \theta = \frac{\pi}{2} \\ 0 & \theta \neq \frac{\pi}{2} \end{cases}$$

Mino time:

$$\tau = \frac{1}{a\sqrt{C(u_+ - u_-)}} F\left(\chi, \frac{u_+}{u_+ - u_-}\right)\Bigg|_{\chi_{\mathrm{s}}}^{\chi_{\mathrm{o}}}$$

Emission intensity

$$I_{\mathrm{emt}}(\boldsymbol{x}) = \begin{cases} f_{\mathsf{d}}(r)\Theta\left(r_{\mathsf{d},+} - r\right)\Theta\left(r - r_{\mathsf{d},-}\right) & \theta = \frac{\pi}{2} \\ 0 & \theta \neq \frac{\pi}{2} \end{cases}$$

Mino time:

$$\tau = \frac{1}{a\sqrt{C(u_+ - u_-)}} F\left(\chi, \frac{u_+}{u_+ - u_-}\right)\Bigg|_{\chi_{\mathrm{s}}}^{\chi_{\mathrm{o}}}$$

$$\cos\theta = \sqrt{u_+}\cos\chi$$

Emission intensity

$$I_{\rm emt}\left(\boldsymbol{x}\right) = \begin{cases} f_{\sf d}(r)\Theta\left(r_{{\sf d},+}-r\right)\Theta\left(r-r_{{\sf d},-}\right) & \theta=\frac{\pi}{2} \\ 0 & \theta\neq\frac{\pi}{2} \end{cases}$$

Mino time:

$$\tau = \frac{1}{a\sqrt{C(u_+-u_-)}}F\left(\chi,\frac{u_+}{u_+-u_-}\right)\Bigg|_{\chi_{\rm s}}^{\chi_{\rm o}}$$

Transfer functions:

$$r_{\rm s} = r_3+\frac{r_4-r_3}{1-\frac{r_{41}}{r_{31}}{\rm sn}^2\left(\pm\frac{\sqrt{Cr_{31}r_{32}}}{2}(\mathcal{I}_r(\xi_{\rm o})-\tau),\frac{r_{32}r_{41}}{r_{42}r_{31}}\right)}$$

$$\cos\theta=\sqrt{u_+}\cos\chi$$

$$\theta_{\rm s} = \arccos\left(\sqrt{u_+}\cos\chi_{\rm s}\right)$$

Emission intensity

$$I_{\rm emt}\left(\boldsymbol{x}\right) = \begin{cases} f_{\sf d}(r)\Theta\left(r_{{\sf d},+}-r\right)\Theta\left(r-r_{{\sf d},-}\right) & \theta=\frac{\pi}{2} \\ 0 & \theta\neq\frac{\pi}{2} \end{cases}$$

Mino time:

$$\tau = \frac{1}{a\sqrt{C(u_+-u_-)}}F\left(\chi,\frac{u_+}{u_+-u_-}\right)\Bigg|_{\chi_{\rm s}}^{\chi_{\rm o}}$$

Transfer functions:

$$r_{\rm s} = r_3+\frac{r_4-r_3}{1-\frac{r_{41}}{r_{31}}{\rm sn}^2\left(\pm\frac{\sqrt{Cr_{31}r_{32}}}{2}(\mathcal{I}_r(\xi_{\rm o})-\tau),\frac{r_{32}r_{41}}{r_{42}r_{31}}\right)}$$

$$\cos\theta=\sqrt{u_+}\cos\chi$$

$$\theta_{\rm s} = \arccos\left(\sqrt{u_+}\cos\chi_{\rm s}\right)$$

where $\mathcal{I}_r(\xi)=\pm\frac{2}{\sqrt{C}\sqrt{r_{31}r_{42}}}F\left(\arcsin\left(\frac{\sinh\xi}{\sqrt{\frac{r_{41}}{r_{31}}\left(\cosh^2\xi-\frac{r_3}{r_4}\right)}}\right),\frac{r_{32}r_{41}}{r_{42}r_{31}}\right)\Bigg|_{\xi_{\rm s}}^{\xi_{\rm o}}$

Emission intensity

$$I_{\mathrm{emt}}(\boldsymbol{x}) = \begin{cases} f_{\mathsf{d}}(r)\Theta\left(r_{\mathsf{d},+}-r\right)\Theta\left(r-r_{\mathsf{d},-}\right) & \theta=\frac{\pi}{2} \\ 0 & \theta\neq\frac{\pi}{2} \end{cases}$$

Mino time:

$$\tau = \frac{1}{a\sqrt{C(u_+-u_-)}} F\left(\chi, \frac{u_+}{u_+-u_-}\right)\Bigg|_{\chi_{\mathrm{s}}}^{\chi_{\mathrm{o}}}$$

Transfer functions:

$$r_{\mathrm{s}} = r_3 + \frac{r_4-r_3}{1-\frac{r_{41}}{r_{31}}\mathrm{sn}^2\left(\pm\frac{\sqrt{Cr_{31}r_{32}}}{2}\left(\mathcal{I}_r(\xi_{\mathrm{o}})-\tau\right), \frac{r_{32}r_{41}}{r_{42}r_{31}}\right)}$$

$$\theta_{\mathrm{s}} = \arccos\left(\sqrt{u_+}\cos\chi_{\mathrm{s}}\right)$$

$$\cos\theta = \sqrt{u_+}\cos\chi$$
$$r = r_4\cosh^2\xi$$

where $\mathcal{I}_r(\xi) = \pm\frac{2}{\sqrt{C}\sqrt{r_{31}r_{42}}} F\left(\arcsin\left(\frac{\sinh\xi}{\sqrt{\frac{r_{41}}{r_{31}}\left(\cosh^2\xi-\frac{r_3}{r_4}\right)}}\right), \frac{r_{32}r_{41}}{r_{42}r_{31}}\right)\Bigg|_{\xi_{\mathrm{s}}}^{\xi_{\mathrm{o}}}$

Emission intensity

$$I_{\mathrm{emt}}(\boldsymbol{x}) = \begin{cases} f_{\mathsf{d}}(r)\Theta\left(r_{\mathsf{d},+} - r\right)\Theta\left(r - r_{\mathsf{d},-}\right) & \theta = \frac{\pi}{2} \\ 0 & \theta \neq \frac{\pi}{2} \end{cases}$$

Mino time:

$$\tau = \frac{1}{a\sqrt{C(u_+ - u_-)}} F\left(\chi, \frac{u_+}{u_+ - u_-}\right)\Bigg|_{\chi_{\mathrm{s}}}^{\chi_{\mathrm{o}}}$$

Transfer functions:

For nth order images: $|\chi_{\mathrm{s}}| = \pi(n + \frac{1}{2})$

$$\cos\theta = \sqrt{u_+}\cos\chi$$
$$r = r_4\cosh^2\xi$$

$$r_{\mathrm{s}} = r_3 + \frac{r_4 - r_3}{1 - \frac{r_{41}}{r_{31}}\mathrm{sn}^2\left(\pm\frac{\sqrt{C r_{31} r_{32}}}{2}(\mathcal{I}_r(\xi_{\mathrm{o}}) - \tau), \frac{r_{32} r_{41}}{r_{42} r_{31}}\right)}$$

$$\theta_{\mathrm{s}} = \arccos\left(\sqrt{u_+}\cos\chi_{\mathrm{s}}\right)$$

where $\mathcal{I}_r(\xi) = \pm\frac{2}{\sqrt{C}\sqrt{r_{31} r_{42}}} F\left(\arcsin\left(\frac{\sinh\xi}{\sqrt{\frac{r_{41}}{r_{31}}\left(\cosh^2\xi - \frac{r_3}{r_4}\right)}}\right), \frac{r_{32} r_{41}}{r_{42} r_{31}}\right)\Bigg|_{\xi_{\mathrm{s}}}^{\xi_{\mathrm{o}}}$

Image of Thin Accretion Disk

Primary, Secondary, and $n = 2$ images: near and distant, Kerr black hole

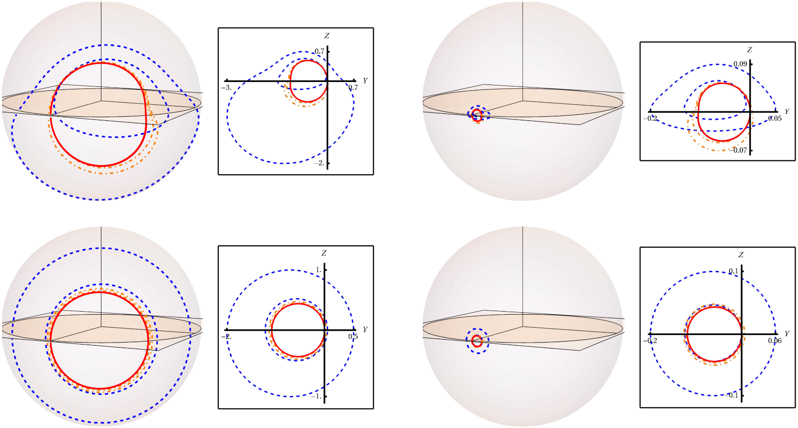

Image of Thin Accretion Disk

Primary, Secondary, and $n = 2$ images: near and distant, Kerr black hole

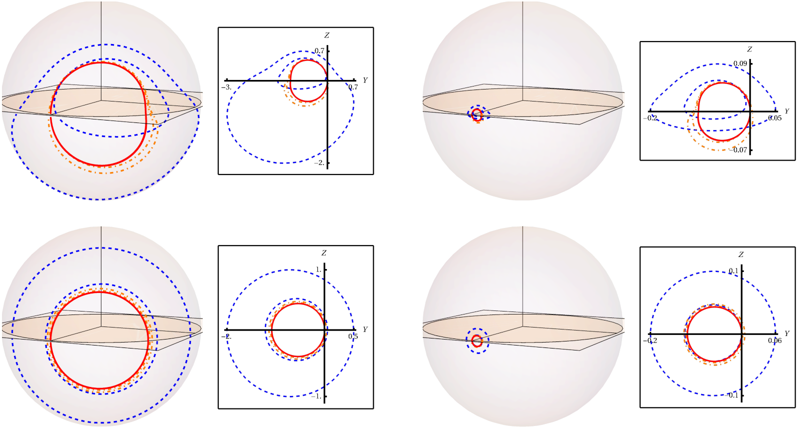

$$r_{\text{obs}} = 10M \, , \theta_{\text{obs}} = 2\pi/5$$

Image of Thin Accretion Disk

Primary, Secondary, and $n = 2$ images: near and distant, Kerr black hole

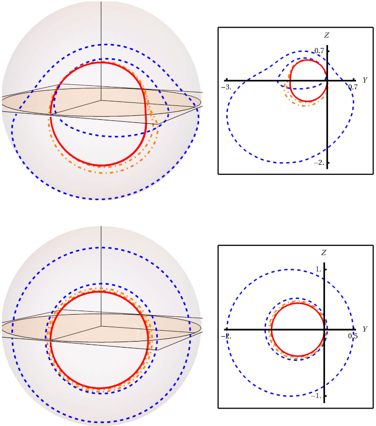

$$r_{\rm obs} = 10M \,, \theta_{\rm obs} = 2\pi/5$$

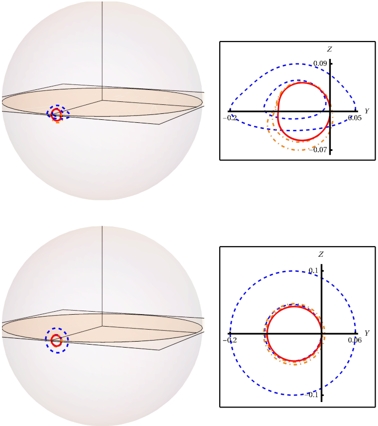

$$r_{\rm obs} = 100M \,, \theta_{\rm obs} = 2\pi/5$$

Image of Thin Accretion Disk

Primary, Secondary, and $n = 2$ images: radial velocities

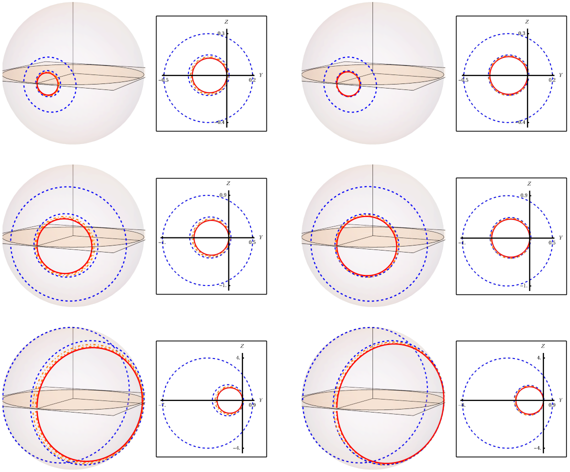

Image of Thin Accretion Disk

Primary, Secondary, and $n = 2$ images: radial velocities

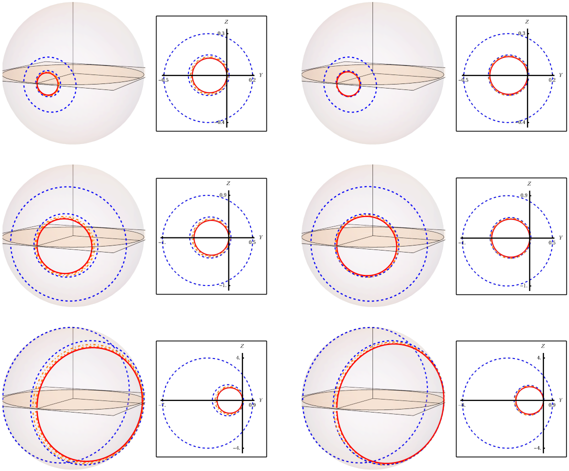

$$a = 0.99M$$

Image of Thin Accretion Disk

Primary, Secondary, and $n = 2$ images: radial velocities

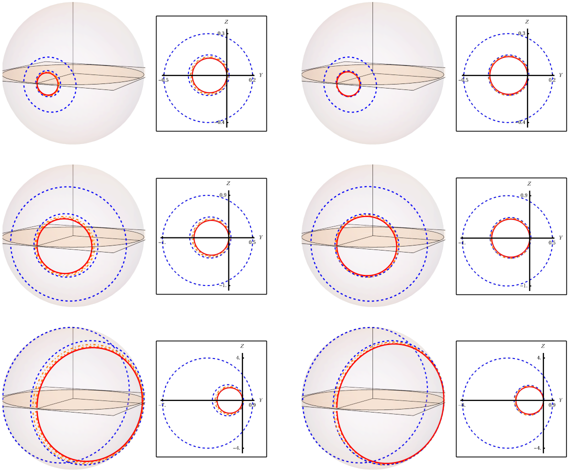

$a = 0.99M$ $a = 0.1M$

Image of Thin Accretion Disk

Primary, Secondary, and $n = 2$ images: radial velocities

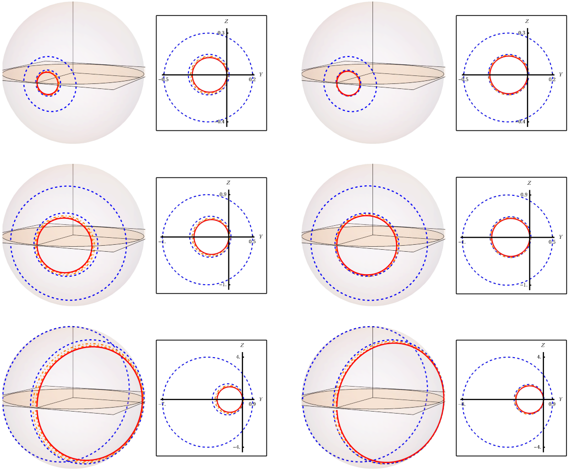

$a = 0.99M$ $\quad$ $a = 0.1M$

in-going geodesic observers

Image of Thin Accretion Disk

Primary, Secondary, and $n = 2$ images: radial velocities

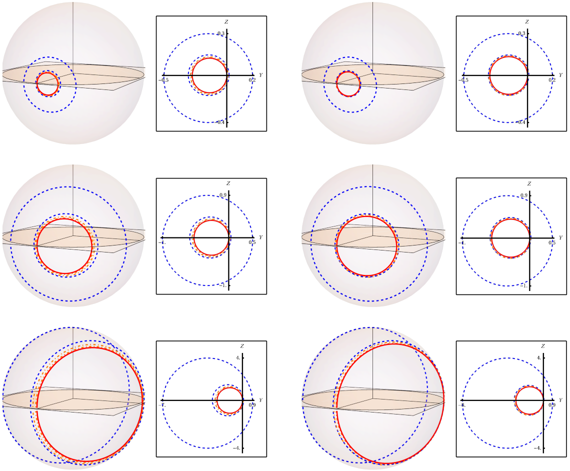

in-going geodesic observers

static observers

$a = 0.99M$ $a = 0.1M$

Image of Thin Accretion Disk

Primary, Secondary, and $n = 2$ images: radial velocities

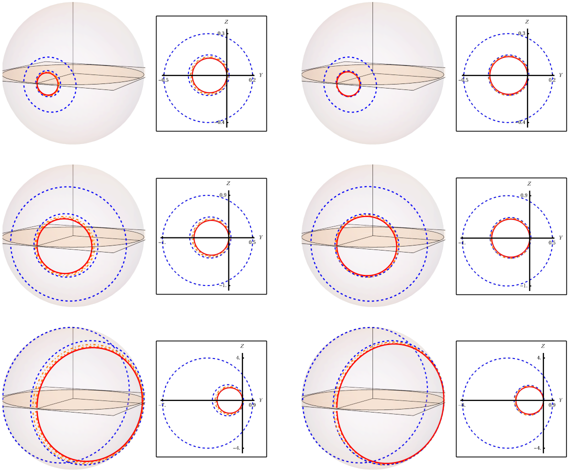

in-going geodesic observers

static observers

out-going geodesic observers

$a = 0.99M$ $\quad$ $a = 0.1M$

Image of Thin Accretion Disk

Primary, Secondary, and $n = 2$ images: axial motions, large inclination angle, near observers

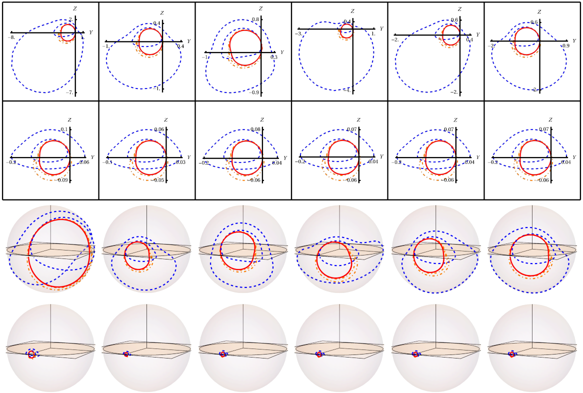

Image of Thin Accretion Disk

Primary, Secondary, and $n = 2$ images: axial motions, large inclination angle, near observers

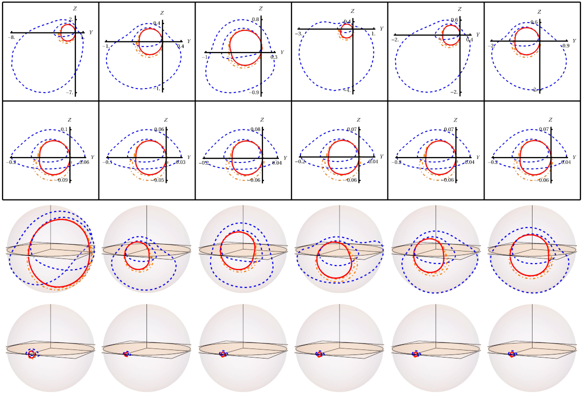

Relative 3-speed:

$$v \equiv \frac{\sqrt{\gamma^* u \cdot \gamma^* u}}{u \cdot u_{\text{ref}}}$$

where $\gamma_{\mu\nu} = g_{\mu\nu} + u_{\text{ref},\mu} u_{\text{ref},\nu}$

Image of Thin Accretion Disk

Primary, Secondary, and $n = 2$ images: axial motions, large inclination angle, near observers

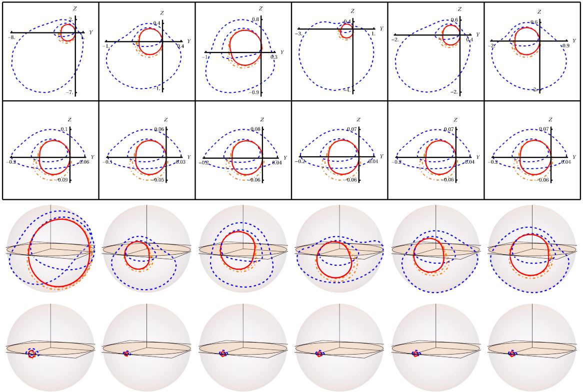

$$r_{\text{obs}} = 10M\ , \theta_{\text{obs}} = 2\pi/5$$

Relative 3-speed:

$$v \equiv \frac{\sqrt{\gamma^* u \cdot \gamma^* u}}{u \cdot u_{\text{ref}}}$$

where $\gamma_{\mu\nu} = g_{\mu\nu} + u_{\text{ref},\mu} u_{\text{ref},\nu}$

Image of Thin Accretion Disk

Primary, Secondary, and $n = 2$ images: axial motions, large inclination angle, near observers

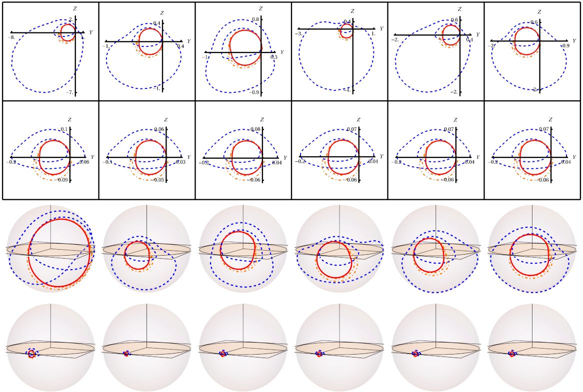

$$r_{\rm obs} = 10M\,,\theta_{\rm obs} = 2\pi/5$$

$$r_{\rm obs} = 100M\,,\theta_{\rm obs} = 2\pi/5$$

Relative 3-speed:

$$v \equiv \frac{\sqrt{\gamma^* u \cdot \gamma^* u}}{u \cdot u_{\rm ref}}$$

where $\gamma_{\mu\nu} = g_{\mu\nu} + u_{{\rm ref},\mu} u_{{\rm ref},\nu}$

Image of Thin Accretion Disk

Primary, Secondary, and $n = 2$ images: axial motions, small inclination angle

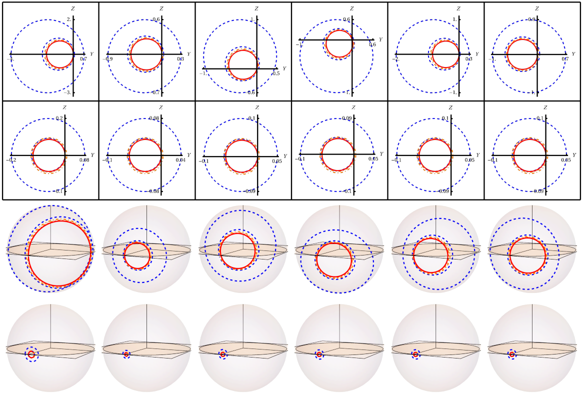

Image of Thin Accretion Disk

Primary, Secondary, and $n = 2$ images: axial motions, small inclination angle

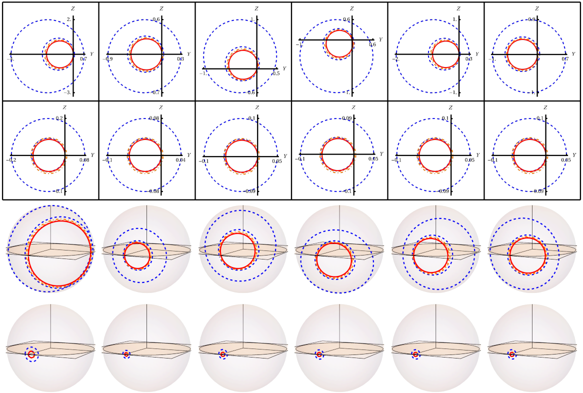

$$r_{\text{obs}} = 10M\ , \theta_{\text{obs}} = \pi/25$$

Image of Thin Accretion Disk

Primary, Secondary, and $n = 2$ images: axial motions, small inclination angle

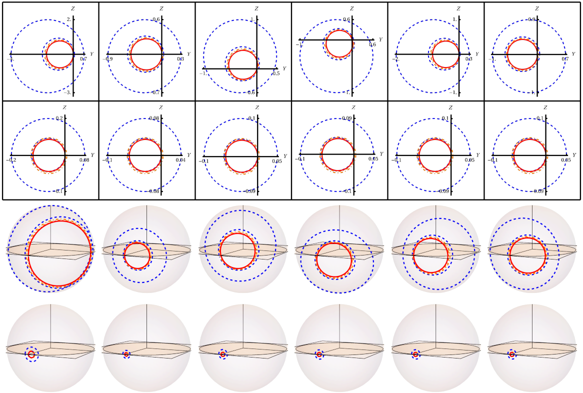

$r_{\rm obs} = 10M\,,\theta_{\rm obs} = \pi/25$

$r_{\rm obs} = 100M\,,\theta_{\rm obs} = \pi/25$

Image of Thin Accretion Disk

Primary, Secondary, and $n = 2$ images: axial motions, cosmological constant

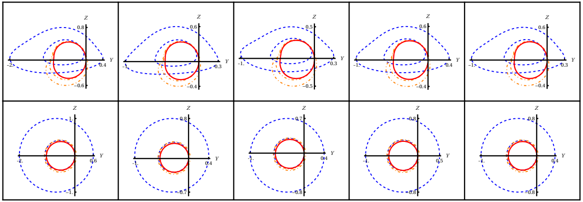

Image of Thin Accretion Disk

Primary, Secondary, and $n = 2$ images: axial motions, cosmological constant

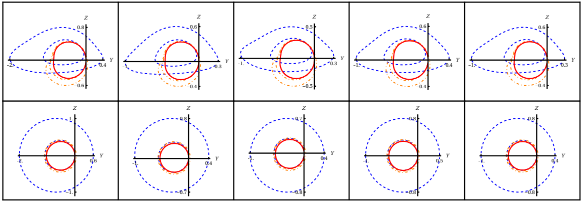

$$r_{\rm obs} = 100M\ ,\theta_{\rm obs} = 2\pi/5$$

Image of Thin Accretion Disk

Primary, Secondary, and $n = 2$ images: axial motions, cosmological constant

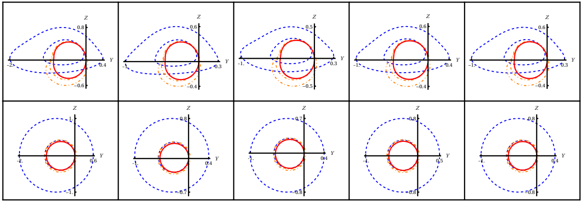

$r_{\text{obs}} = 100M$, $\theta_{\text{obs}} = 2\pi/5$

$r_{\text{obs}} = 100M$, $\theta_{\text{obs}} = \pi/25$

Image of Thin Accretion Disk

Primary, Secondary, and $n = 2$ images: cosmological constant, near outer horizon, co-moving frame

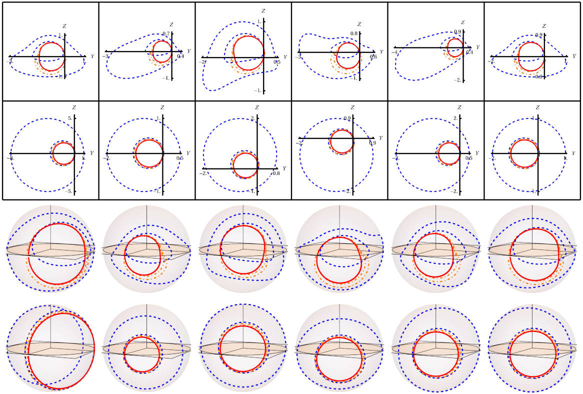

Image of Thin Accretion Disk

Primary, Secondary, and $n = 2$ images: cosmological constant, near outer horizon, co-moving frame

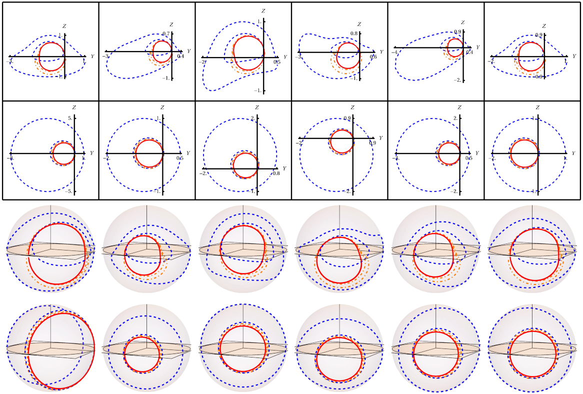

$$r_{\mathrm{obs}} = 16M\ , \theta_{\mathrm{obs}} = 2\pi/5$$

Image of Thin Accretion Disk

Primary, Secondary, and $n = 2$ images: cosmological constant, near outer horizon, co-moving frame

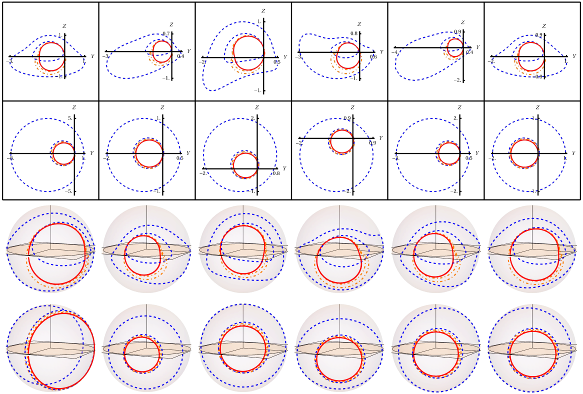

$$r_{\rm obs} = 16M\,,\theta_{\rm obs} = 2\pi/5$$

$$r_{\rm obs} = 16M\,,\theta_{\rm obs} = \pi/25$$

Image of Thin Accretion Disk

Primary, Secondary, and $n = 2$ images: cosmological constant, near outer horizon, co-moving frame

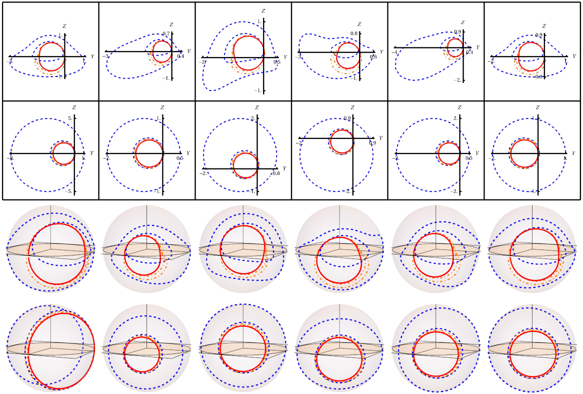

$$r_{\mathrm{obs}} = 16M\ , \theta_{\mathrm{obs}} = 2\pi/5$$

$$r_{\mathrm{obs}} = 16M\ , \theta_{\mathrm{obs}} = \pi/25$$

Outer horizon: $r_{\mathrm{H}} \simeq 16.2M$,

with respect to co-moving frame

Primary, Secondary, and $n = 2$ images: cosmological constant, near outer horizon, static frame

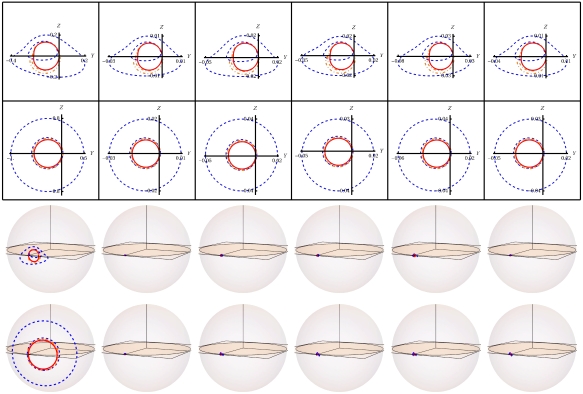

Outer horizon: $r_{\mathrm{H}} \simeq 16.2M$

Image of Thin Accretion Disk

Primary, Secondary, and $n = 2$ images: cosmological constant, near outer horizon, static frame

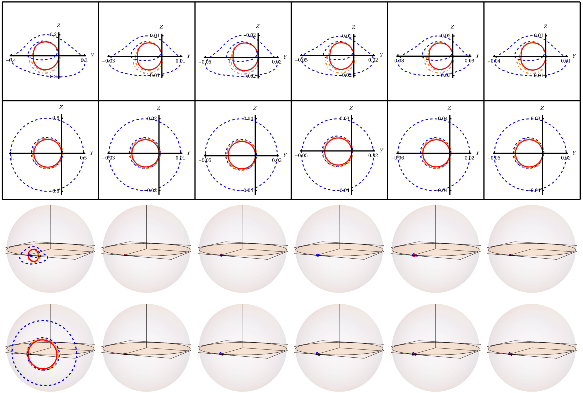

$r_{\rm obs} = 16M \, , \theta_{\rm obs} = 2\pi/5$

Outer horizon: $r_{\rm H} \simeq 16.2M$

Image of Thin Accretion Disk

Primary, Secondary, and $n = 2$ images: cosmological constant, near outer horizon, static frame

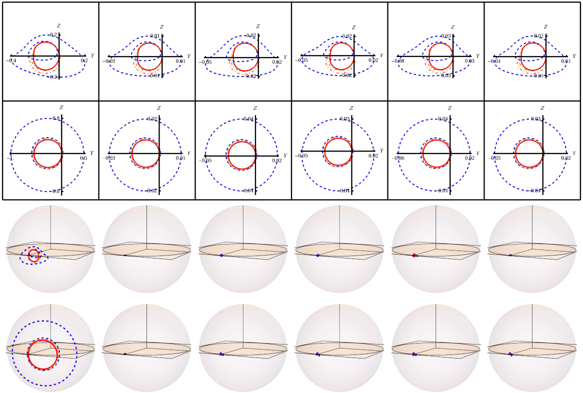

$r_{\text{obs}} = 16M\,, \theta_{\text{obs}} = 2\pi/5$

$r_{\text{obs}} = 16M\,, \theta_{\text{obs}} = \pi/25$

Outer horizon: $r_{\text{H}} \simeq 16.2M$

Image of Thin Accretion Disk

Primary, Secondary, and $n = 2$ images: cosmological constant, near outer horizon, static frame

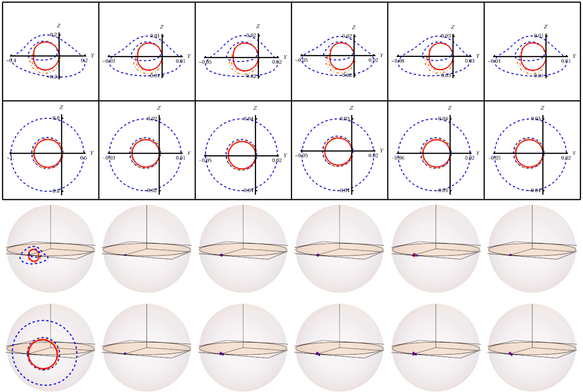

$r_{\rm obs} = 16M$, $\theta_{\rm obs} = 2\pi/5$

$r_{\rm obs} = 16M$, $\theta_{\rm obs} = \pi/25$

Outer horizon: $r_{\rm H} \simeq 16.2M$

with respect to static frame

Image of Thin Accretion Disk

Primary, Secondary, and $n = 2$ images: Size

Size of the images:

$$Z_{\text{size}} \equiv \frac{(Z_{\max} - Z_{\min})|_{\upsilon}}{(Z_{\max} - Z_{\min})|_{\upsilon=0}} \ .$$

Size of the images:

$$Z_{\text{size}} \equiv \frac{(Z_{\max} - Z_{\min})|_{\upsilon}}{(Z_{\max} - Z_{\min})|_{\upsilon=0}} \ .$$

Schematic diagram:

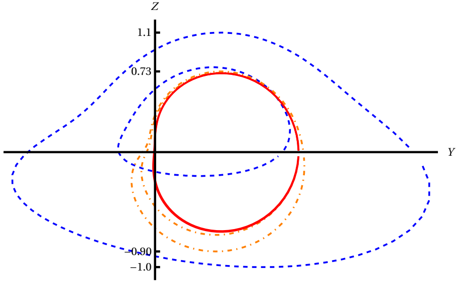

Size of the images:

$$Z_{\text{size}} \equiv \frac{(Z_{\text{max}} - Z_{\text{min}})|_{\upsilon}}{(Z_{\text{max}} - Z_{\text{min}})|_{\upsilon=0}} .$$

Schematic diagram:

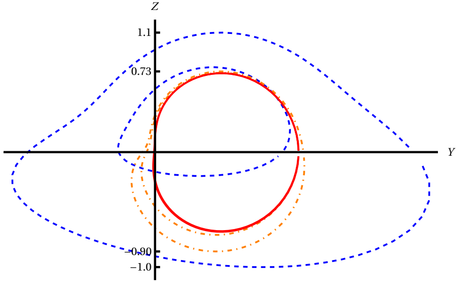

One can derive:

$$Z_{\text{size}} = \frac{\tan \Psi'}{\tan \Psi}$$

Size of the images:

$$Z_{\text{size}} \equiv \frac{(Z_{\text{max}} - Z_{\text{min}})|_{\upsilon}}{(Z_{\text{max}} - Z_{\text{min}})|_{\upsilon=0}} .$$

Schematic diagram:

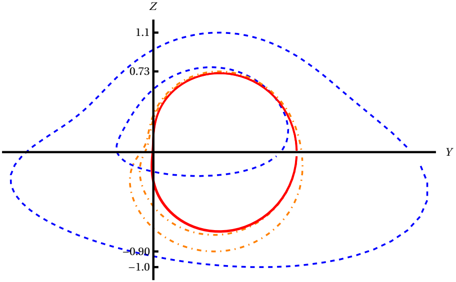

One can derive:

$$Z_{\text{size}} = \frac{\tan \Psi'}{\tan \Psi} \overset{??}{=} \sqrt{\frac{1-v}{1+v}}$$

Image of Thin Accretion Disk

Size of Primary, Secondary, and $n = 2$ images: in-going radial motion, small inclination angle, near and distant observers.

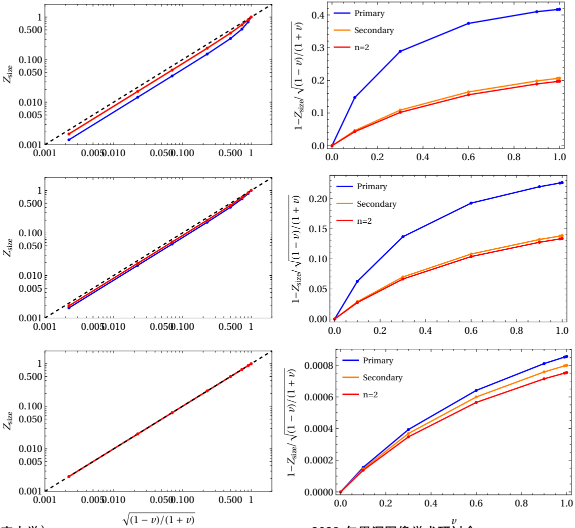

Image of Thin Accretion Disk

Size of Primary, Secondary, and $n = 2$ images: in-going radial motion, small inclination angle, near and distant observers.

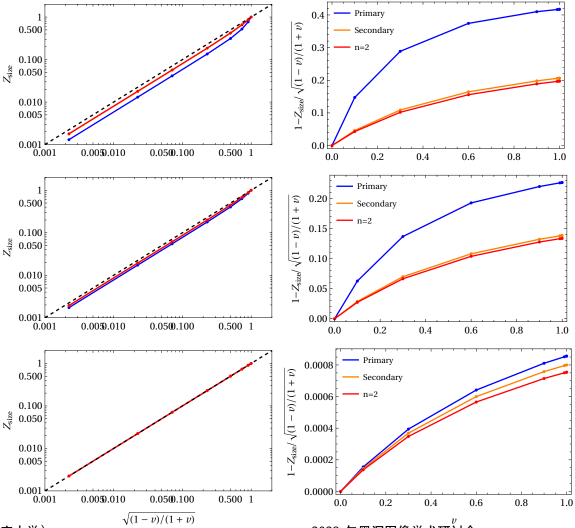

$r_{\rm obs} = 10M$, Kerr-de Sitter

Image of Thin Accretion Disk

Size of Primary, Secondary, and $n = 2$ images: in-going radial motion, small inclination angle, near and distant observers.

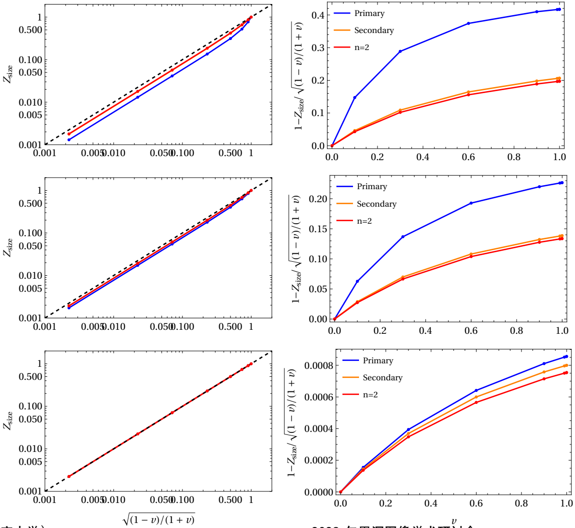

$r_{\rm obs} = 10M$, Kerr-de Sitter

$r_{\rm obs} = 10M$, Kerr

Image of Thin Accretion Disk

Size of Primary, Secondary, and $n = 2$ images: in-going radial motion, small inclination angle, near and distant observers.

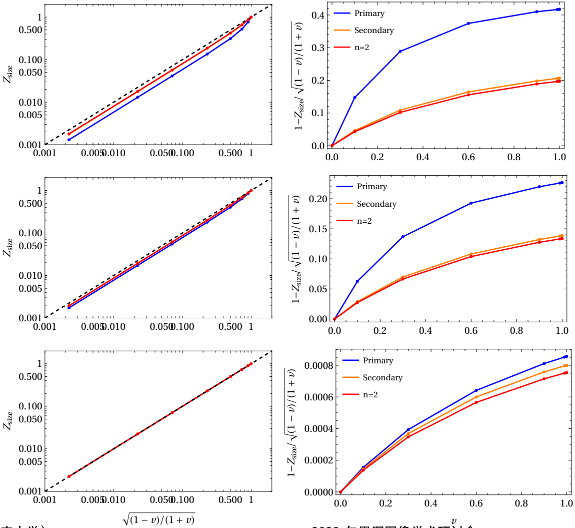

$r_{obs} = 10M$, Kerr-de Sitter

$r_{obs} = 10M$, Kerr

$r_{obs} = 100M$, Kerr

Image of Thin Accretion Disk

Size of Primary, Secondary, and $n = 2$ images: axial motion, small inclination angle, near observers.

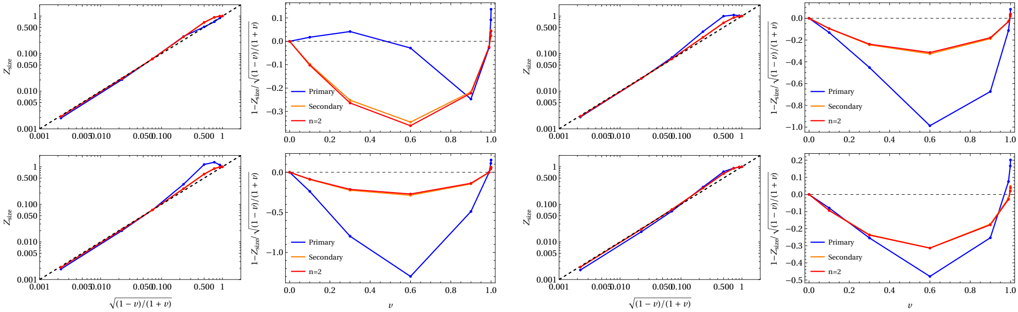

Image of Thin Accretion Disk

Size of Primary, Secondary, and $n=2$ images: axial motion, small inclination angle, near observers.

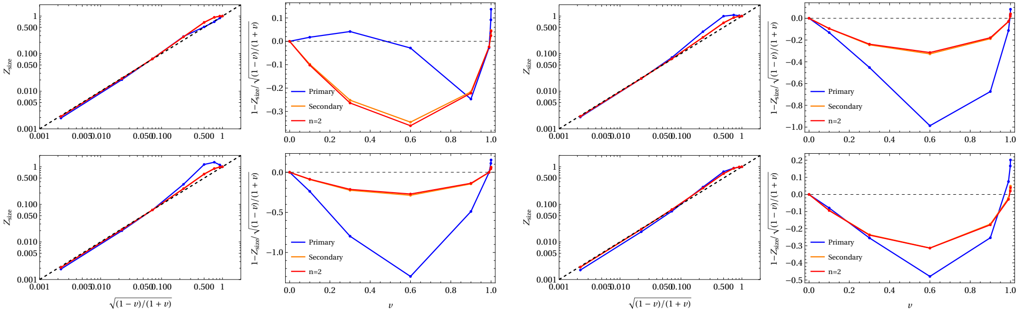

$$r_{\rm obs} = 10M\ ,\ u^{(\phi,\mp)}$$

Image of Thin Accretion Disk

Size of Primary, Secondary, and $n = 2$ images: axial motion, small inclination angle, near observers.

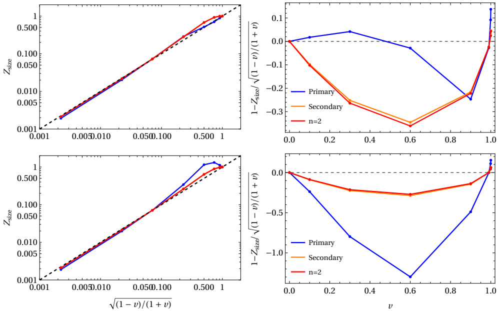

$$r_{\rm obs} = 10M\ ,\ u^{(\phi,\mp)}$$

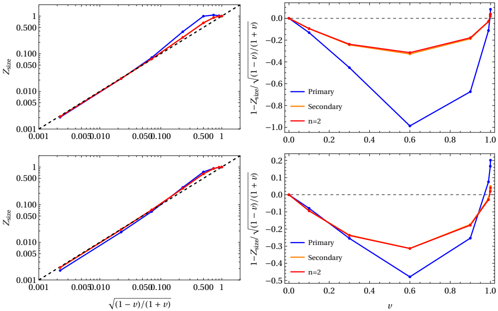

$$r_{\rm obs} = 10M\ ,\ u^{(\theta,\mp)}$$

Summary

- The key question is: whether the distinctions in the images induced by the aberration effect are simply kinematic effects or can reflect the spacetime geometries.

Summary

- The key question is: whether the distinctions in the images induced by the aberration effect are simply kinematic effects or can reflect the spacetime geometries.

  It is true, but only from the qualitative studies.

Summary

- The key question is: whether the distinctions in the images induced by the aberration effect are simply kinematic effects or can reflect the spacetime geometries.

  It is true, but only from the qualitative studies.

- Whether the distinct behaviors of different order images can offer a way to investigate both space-time geometries and emissions separately.

Thank you!

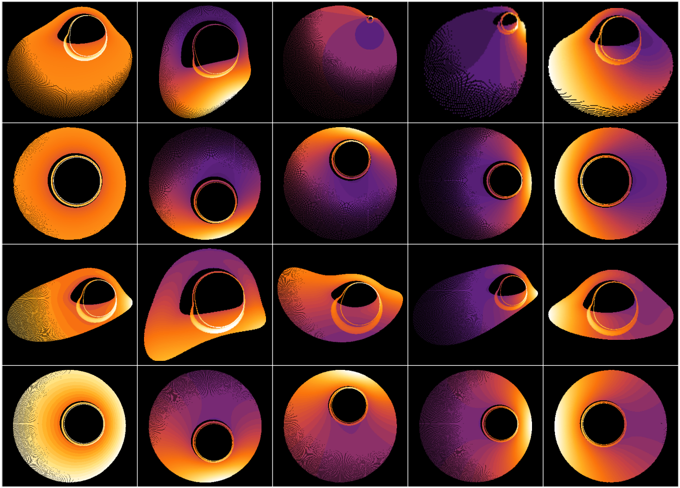

Thank you!